LAWRENCE
LIVERMORE
NATIONAL
LABORATORY

UCRL-JRNL-228082

Morphological tranformation of calcite crystal growth by prismatic "acidic" polypeptide sequences.

I. Kim, J. L. Giocondi, C. A. Orme, J. Collino, J. S. Evans

February 15, 2007

Crystal Growth and Design

Disclaimer

Morphological tranformation of calcite crystal growth by prismatic "acidic" polypeptide sequences.

Il Won Kim,[1] Jennifer L. Giocondi,[2] Christine Orme,[2] Sebastiano Collino,[1] and John Spencer Evans[1*]

[1]Laboratory for Chemical Physics, Center for Biomolecular Materials Spectroscopy, New York University, 345 E. 24th Street, Room 1007, New York, New York, 10010, and [2]Department of Chemistry and Materials Science, Lawrence Livermore National Laboratory, Livermore, CA 94551.

*to whom correspondence should be addressed. Tel: 2129989605

Fax: 2129954087

Email: jse1@nyu.edu

Abbreviations: CD: circular dichroism; AFM: atomic force microscopy

ABSTRACT Many of the interesting mechanical and materials properties of the mollusk shell are thought to stem from the prismatic calcite crystal assemblies within this composite structure. It is now evident that proteins play a major role in the formation of these assemblies. Recently, a superfamily of 7 conserved prismatic layer-specific mollusk shell proteins, Asprich, were sequenced, and the 42 AA C-terminal sequence region of this protein superfamily was found to introduce surface voids or porosities on calcite crystals *in vitro*. Using AFM imaging techniques, we further investigate the effect that this 42 AA domain (Fragment-2) and its constituent subdomains, DEAD-17 and Acidic-2, have on the morphology and growth kinetics of calcite dislocation hillocks. We find that Fragment-2 adsorbs on terrace surfaces and pins acute steps, accelerates then decelerates the growth of obtuse steps, forms clusters and voids on terrace surfaces, and transforms calcite hillock morphology from a rhombohedral form to a rounded one. These results mirror yet are distinct from some of the earlier findings obtained for nacreous polypeptides. The subdomains Acidic-2 and DEAD-17 were found to accelerate then decelerate obtuse steps and induce oval rather than rounded hillock morphologies. Unlike DEAD-17, Acidic-2 does form clusters on terrace surfaces and exhibits stronger obtuse velocity inhibition effects than either DEAD-17 or Fragment-2. Interestingly, a 1:1 mixture of both subdomains induces an irregular polygonal morphology to hillocks, and exhibits the highest degree of acute step pinning and obtuse step velocity inhibition. This suggests that there is some interplay between subdomains within an intra (Fragment-2) or intermolecular (1:1 mixture) context, and sequence interplay phenomena may be employed by biomineralization proteins to exert net effects on crystal growth and morphology.

INTRODUCTION

The mollusk shell offers some interesting building principles for crystal growth and the design of new high performance composite inorganic/organic materials.[1-5] Primarily, the research focus has been on the nacreous or aragonite layer of the shell, since this layer offers two very interesting materials paradigms: polymorph selection/stabilization and fracture resistance.[4-8] However, in some mollusks there exists another shell layer, termed the prismatic layer, which is formed from the calcium carbonate polymorph, calcite. This layer features a parallel assembly of long calcite prisms, which appears to be single crystals but may be comprised of many nanometer-sized grains with the same crystal orientation.[6,7] The prismatic layer is more brittle than the nacreous layer, and experiences radial crack propagation when subject to indentations, which could be useful for puncture resistance.[6] The proteins which comprise the prismatic layer are believed to play a major role in establishing these properties.[6,7,9-11] To date, only a handful of prismatic – associated proteins have been identified and completely sequenced.[12-14] These proteins are unusual, in that they possess polyanionic sequence domains and/or repetitive sequence blocks,[12-14] and, exist as occluded species within the mineral phase.[9-14] Unfortunately, very little is known about these proteins or about the mechanism(s) involved in prismatic protein – mediated crystal growth and design within the mollusk shell. This lack of knowledge hampers our ability to understand and exploit the molecular features of these proteins for materials synthesis strategies.

Recently, a superfamily of seven prismatic layer – associated proteins from the mollusk *Atrina rigida*, termed Asprich, were identified and sequenced.[12] The presence of

highly conserved N- and C-terminal sequence domains within this superfamily indicates that these sequences are critical to Asprich function and probably play a role in prismatic crystal growth and architecture.[12] To determine if these conserved sequences could modulate calcium carbonate nucleation and crystal growth, we initially tested the Asprich 42 AA C-terminal domain, termed Fragment–2 (Figure 1),[16] for its ability to control calcite crystal growth *in vitro*.[15] Fragment-2 is oberved to induce porosities or voids on the surfaces of rhombohedral calcite crystals; its integral subdomains, the 17-AA DEAD-17 and 25-AA Acidic-2 subdomains (Figure 1), also limit crystal growth, leading to unequal crystal growth patterns on rhombohedral crystal surfaces, but do not induce porous regions on crystal surfaces.[15] The structure of all three sequences are very similar, i.e., they exist in a conformational equilibrium with random coil and polyproline Type II structures (PPII),[15] and these structural features are believed to have an impact on the functionality of these sequences.

At this stage it is not clear how Fragment-2 or its associated subdomains control calcite crystal growth. Restricting crystal growth could represent part of a building strategy that is utilized by the Asprich superfamily to construct aligned prismatic crystals, to control the cross-sectional dimensions of these crystals within the mollusk shell, or, to create nanometer-sized grains within the calcite prisms.[6] To better understand this process, we performed *in situ* atomic force microscopy (AFM) studies of Fragment-2, Acidic-2, and DEAD-17 polypeptides and their effect on calcite growth by monitoring the growth of dislocation hillocks on geologic calcite fragments.[17,18] Here, our primary aim is to determine whether or not Fragment-2 and its subdomains affect crystal growth at specific hillock regions. Our secondary aim is to compare the performance of these prismatic layer –

specific sequences with previously published studies[17] involving nacreous sequences, n16N, AP7N, and AP24N, that are derived from the N-terminal regions of nacre-layer proteins, n16,[19] AP7,[20] and AP24,[20] respectively. Our AFM experiments indicate that Fragment-2 and its associated subdomains transform crystal morphology and growth kinetics in ways that are partly similar to but distinctly different from nacreous sequences.[17] Using circular dichroism (CD) we also find that the conformation of Fragment-2 and its subdomains is not sensitive to the presence of Ca (II); in fact, all three polypeptides maintain their unfolded conformational state in the presence of Ca (II) and retain PPII and random coil structural features. However, our most interesting finding has to do with the individual mineralization traits of Acidic-2 and DEAD-17 and how these trait metamorphose under certain conditions: the crystal growth properties of the individual DEAD-17 and Acidic-2 subdomains are substantially modified when both domains are present together as colinear partners, or, when present together as a mixture of individual species. We believe that the observed interplay between DEAD-17 and Acidic-2, as well as the structural features of these subdomains, are critical to the function of the C-terminal domain of Asprich.

MATERIALS AND METHODS

In Situ AFM. N^{α}-acetyl-capped, free C-terminal Fragment-2, Acidic-2, and N^{α}-acetyl-, C^{α}-amide capped DEAD-17 were synthesized and purified as described previously.[15] Both peptides were synthesized at the 100 micromole level and purified at the Wm. Keck Biotechnology Peptide Synthesis Facility, Yale University, by Dr. Janet Crawford. AFM experiments were performed on surfaces of anchored calcite crystals (freshly cleaved geologic calcite from Brazil, ≤ 1 mm each dimension) that were subjected to overgrowth

via exposure to a supersaturated solution of $CaCl_2$/$NaHCO_3$ (2.5 mM $CaCl_2$, 2.5 mM $NaHCO_3$ in deionized distilled water) and imaged in real time using an atomic force microscope outfitted with a commercially available fluid cell (Nanoscope III, Digital Instruments, Santa Barbara, CA).[16-18] Prior to peptide introduction into the fluid cell system, each calcite crystal was equilibrated via exposure to supersaturated solution; the choice of flow rate (1 mL/min) was such that step kinetics were not limited by bulk diffusion. Once well-defined hillocks were detected, polypeptides were then introduced using a freshly prepared supersaturated solution at the same flowrate. This solution consisted of a given peptide dissolved in $NaHCO_3$ solution, which was filtered using a 0.2 μM PVDF Gelman Acrodisc[17] and then mixed with $CaCl_2$ solution, with the final concentration of both $CaCl_2$ and $NaHCO_3$ = 2.5 mM and the final peptide concentration = 3, 6, or 12 μM. Negative control conditions utilized supersaturated solutions that were devoid of any added peptide; these solutions normally have a pH of 8.3, and therefore were adjusted to 8.1 by adding minute amount of concentrated dilute aqueous HCl. The addition of polypeptides to the unadjusted negative control solution (pH = 8.3) led to an approximate 0.2 unit downshift to pH 8.1. Thus, in all cases, the final pH of all solutions was 8.1 to avoid downshift in supersaturation or slowing of step growth kinetics. For this pH range the supersaturation ratio ($S = [(Ca^{2+})(CO_3^{2-})]/K_{sp,CaCO3}$) and the ionic ratio ($\{Ca^{2+}\}/(CO_3^{2-}\}$) of pure solutions (no polypeptide) were computed using Geochemists' Workbench software (v.5, Rockware, Inc.) and found vary between 6.1 - 9.5 and 130 - 80, respectively. For mixing studies involving Acidic-2 and DEAD subdomains, these peptides were mixed together in a 1 : 1 mole ratio in $NaHCO_3$ at the start of the experiment, with final individual peptide concentrations = 3, 6, or 12 μM. All imaging was performed on the {104} cleavage plane of calcite.

AFM fluid cell imaging was performed at room temperature with image collection commencing 5 minutes after the introduction of each polypeptide. *In situ* images were collected in contact mode using Si_3N_4 tips and were limited to regions undergoing step growth at dislocation hillocks of calcite. The imaging force was reduced to the minimum possible value that allowed the tip to remain in contact with the surface, such that there was no measurable effect on the growth kinetics.[17] AFM imaging was typically performed once with a given polypeptide sample, and no local erosion or local enhancement of step velocities was observed due to tip effects. Note that step-angle distortion exists in the images because the step front advances during the scan time. Images reported here are not corrected for this effect.[17] All images were processed with Image SXM (version 174-1X) for color, brightness, contrast adjustment and examination of height profile. Dry imaging of calcite crystals exposed to Fragment-2 were obtained by first removing the crystal from the fluid cell, rinsing the crystal with 10 mL of deionized distilled water and dried with clean compressed nitrogen gas. Samples were then imaged in tapping mode using Dimension 3100 AFM instrument. Final image adjustment for all samples was made using Adobe Photoshop.

We monitored the changes of the obtuse step velocity *in situ* caused by the addition of polypeptides to the fluid cell. To circumvent the technical problem accompanied by the significant changes in hillock shape, rather than monitor the obtuse steps directly, we instead monitored the advance of the obtuse – obtuse corner (i.e., corner formed by the inersection of the two obtuse steps) of the dislocation hillocks as a function of time. This velocity was determined by dividing the advance distance measured in the direction that connects acute-acute and obtuse-obtuse corners by the travel time calculated by AFM scan

rates. The obtuse-obtuse corner velocity is approximately 1.4 times the actual obtuse step velocity itself.

Finally, to provide a comparative numerical value of the hillock region, we calculated a hillock shape factor (HSF), which is an approximate number that estimates the hillock shape. This should be considered only as a rough estimate because of the slight difference in the AFM tip scan rate. The HSF value is simply the long axis length (acute-acute to obtuse-obtuse direction) divided by the short axis length (acute-obtuse to acute-obtuse direction) of the hillock. Thus, as the hillock deviates from the rhombohedral shape and elongates, the HSF value will increase.

Circular Dichroism (CD) Spectrometry. CD spectra were obtained for DEAD-17, acidic-2, and DEAD-acidic-2 at 25°C, using an AVIV 60 CD Spectrometer (60DS software version 4.1t). The CD spectrometer was previously calibrated with d-10-camphorsulfonic acid. The peptide samples (apo form) were dissolved and diluted to final concentrations of 12 μM in 100 μM Tris HCl (pH 7.5). In addition, the apo-samples were separately titrated with pH neutralized 99.99% pure $CaCl_2$*$2H_2O$ (Sigma/Aldrich Chemicals, in deionized distilled water) stock solution over a peptide : metal (II) stoichiometry range of 1:1, 1:2, 1:4, 1:10, and 1:20. For all spectra, wavelength scans were conducted from 185 to 260 nm with appropriate background buffer subtraction, using total 3 scans with 1 nm bandwidth and 0.5 nm/sec scan rate[15,19,20] In all CD spectra, mean residue ellipticity [θ_M] is expressed in deg·cm^2·dmol^{-1}.[15,19,20]

RESULTS

AFM studies of Fragment-2. In the absence of polypeptides, atomic force microscopy on the {104} cleavage plane of calcite reveals that growth occurs by advancement of atomic seps emanating from dislocations for the range of supersaturations used in these experiments. Such growth produces hillocks with atomic step directions that reflect typical rhombohedral calcite crystal morphology with step risers along four of the six crystallographically equivalent {104} facets (Figure 2A). Two of the steps are typically termed "acute" (top portion of Figure 2A) due to the acute angle that the step riser makes with respect to the cleavage plane, and two of the steps are termed "obtuse" (bottom portion of Figure 2A) due to the obtuse angle the step riser makes with respect to the cleavage plane.[17,18] Because imaging occurs while the crystal is growing, step kinetics can be directly measured from sequences of images.[17,18]

As shown in Figure 2B, the introduction of Fragment-2 produces several significant effects on calcite dislocation hillock morphology, compared to the negative control condition. First, we observe that the growth front along the obtuse – obtuse step boundaries is "finger-like" and uneven. As shown in Figure 5A, obtuse step velocities are initially accelerated relative to the negative control assay but then decelerate as a function of distance from the dislocation source. We will enlarge upon this in the discussion section. Second, the morphology of acute-obtuse corner sites becomes rounded, losing the sharp delineation between acute and obtuse step directions. It now appears that new step directions are also emerging (Figure 2). Third, we observe acute step "bunching" as noted by the appearance of roughened acute step edges that are not observed in the negative

control scenario. The net effect of Fragment-2 on hillock morphology is a shift from a rhombohedral geometry to a more round geometry with ragged steps (Figure 3, 7) and a HSF value of 1.1. It appears that this morphological shift arises from the adsorption of Fragment-2 onto terrace surfaces of the hillock, which leads to pinning of acute steps, partial pinning of obtuse steps, and modification of corner region morphologies. The greater degree of pinning of the acute steps versus obtuse steps likely occurs due to closer spacing of acute steps. Interactions with the peptide cause the acute steps to deviate from straight lines, and when the amplitude of step wandering becomes comparable with the step spacing, the acute steps begin to interact with one another and create step bunches that are prone to pinning. It does not appear that the peptides bind preferentially to the acute steps, but rather that the acute steps are more affected due to the geometry of the hillock.

The adsorption of Fragment-2 onto terrace surfaces was examined in more detail (Figure 2B). A comparison of calcite dislocation hillock features in the presence of 3 μM and 6 μM Fragment-2 reveals the peptide concentration-dependency which manifests as an overall increase in surface roughening as a function of Fragment-2 concentration, a corresponding increase in pore or void regions, and an increase in cluster density on the terrace surfaces (Figure 2). We note that void or pore formation was originally noted in our SEM studies of Fragment-2 – mediated calcite crystal growth.[15] The source of the surface roughening appears to be the result of cluster formation on terrace surfaces. These clusters are clearly evident in the dry topographic AFM image taken at the end of the *in situ* experiment (Figure 2), where improved resolution in the absence of water reveals these features more clearly. The fact that these features are not readily observed *in situ* suggests that the clusters are probably forming a dense layer or film over the terrace surfaces,

making their surface detection difficult by AFM, which relies on topographic variation. Cluster or deposit formation was also observed for several nacre polypeptide sequences[17] and may represent the formation of hydrated peptide – mineral composites on the terrace surfaces.

AFM studies of individual Acidic-2 and DEAD-17 subdomains. We next examined the individual effects that DEAD-17 and Acidic-2 subdomains exert on calcite hillock growth and morphology (Figure 3). In general, we note that DEAD-17 has the smallest effect on hillock morphology, as evidenced by passing of acute steps and absence of step "bunching" as witnessed for Fragment-2 (Figure 3). DEAD-17 mirrors the ability of Fragment-2 to alter the morphology of acute-obtuse corner regions and promote new step directions, to induce uneven or "finger-like" regions at obtuse step boundaries, and promote initial acceleration of obtuse step velocites near the dislocation source (Figures 3, 5). However, some distinctions should be noted with regard to DEAD-17. First, DEAD-17 has a more pronounced effect on the acute – obtuse corner leading to a more oval hillock morphology (Figure 3). Here, the HSF value = 1.3, which represents an 18% increase in elongation over the Fragment-2 value. Second, compared to Fragment-2, DEAD-17 elicits greater reduction in obtuse – obtuse corner velocities at farther distances from the dislocation source (Figure 5) but not in a concentration-dependent fashion. Finally, we do not observe surface cluster formation in the presence of DEAD-17 (Figure 3).

In comparison to DEAD-17, the Acidic-2 subdomain exhibits more significant effects on calcite hillock growth and morphology. As shown in Figure 3, this subdomain adsorbs onto terrace surfaces and initiates acute step edge "bunching", a feature not observed for

DEAD-17. Acidic-2 also induces irregular, uneven morphology at former acute-obtuse corner regions to a greater degree compared to DEAD-17. The formation of the "finger-like" extensions at obtuse steps appears more extensive (Figure 3) and may arise from small regions of each step that are overcoming the pinning effects of Acidic-2 while the rest of the step essentially stops growing. This is clearly observed in sequential images of calcite dislocation hillocks exposed to Acidic-2 (Figure 4), where one can trace the progression of finger formation at obtuse step edge regions. Compared to Fragment-2 and DEAD-17, Acidic-2 induces a morphological transition in hillocks, shifting from the rhombohedral form to a more elongated oval form (Figure 3, 7). Here, the HSF value = 1.9, which reflects a 73% increase in elongation over the Fragment-2 value. Unlike DEAD-17, Acidic-2 decelerates obtuse step velocities to a greater extent (Figure 5) and in a concentration-dependent fashion. We also note that Acidic-2 induces the formation of cluster deposits visible on crystal terraces (Figure 3), a trait shared with Fragment-2 but not observed for DEAD-17.

Combinatorial mixing experiments involving Acidic-2 and DEAD-17. We initially noted in our earlier studies[15] that the crystal growth properties of DEAD-17 and Acidic-2 subdomains change when both subdomains are combined together in a 1:1 mole ratio mixture within the same assay system.[15] Based upon these findings, and, our observations that DEAD-17 and Acidic-2 effects on calcite hillock growth differ from the parent Fragment-2 sequence (Figure 3, 7), we performed AFM imaging of calcite dislocation hillocks in the presence of 1:1 mole mixture of the two subdomains (Figure 3). Here, we observe that the 1:1 mixture induces pinning of acute steps, uneven, irregular obtuse steps, deceleration in obtuse step velocities (Figure 5), and substantial alteration of acute-obtuse corner morphologies. Note

that these effects are more dramatic than what we observe for Fragment-2 alone and somewhat mirror the situation that occurs in the presence of the Acidic-2 subdomain. We also observe that this polypeptide mixture induces a roughening of terrace surfaces (Figure 2), probably as a result of peptide-mineral cluster formation on these surfaces. The net effect of the 1:1 mixture on calcite hillock morphology is a transition from the rhombohedral form to highly irregular polygonal form (Figure 3). Here, the HSF value = 1.8, which represents a 64% increase in elongation compared to the Fragment-2 value. From these results, we conclude that the mineralization behavior of the 1:1 subdomain mixture differs in a number of significant aspects from Fragment-2 and its individual subdomains.

Asprich sequence conformation in the presence of Ca (II). Given that Fragment-2 possesses a significant percentage of Asp and Glu residues,[12,15] we expected that Ca (II) interaction at these sites might sponsor some degree of conformational change in Fragment-2, which, in turn, could affect the function of this sequence. To address this issue, we performed circular dichroism experiments on Fragment-2 and its associated subdomains in the presence of Ca (II)(Figure 5). Here, in the apo state, we note that all three peptides exhibit similar global conformational spectral signatures, i.e., the presence of a major (-) ellipticity band ($\pi - \pi^*$ transition) at 198 nm, corresponding to random coil or unstructured conformation, and, the presence of a minor, (+) band ($n - \pi^*$ transition) centered near 218 – 220 nm, corresponding to polyproline Type II extended helical conformation.[15,22] To our surprise, we do not observe any significant wavelength shift in either of these ellipticity bands for any of the three peptides in the presence of Ca (II). The absence of a wavelength shift indicates that there is no significant metal-dependent conformational perturbation occuring in any of the peptides in this study. Thus, neither Fragment-2 nor its subdomains

adopt different secondary structures in the presence of Ca (II). Rather, they maintain open, unfolded conformations similar to those adopted in the apo-state,[15] and, PPII structural features are preserved. We conclude that unfolded conformational state and PPII structure both persist in Ca (II) rich environments, and, that these structural features are probably critical for Fragment-2 - mediated mineralization effects noted in our *in vitro* study. We note thatn previous studies conducted with Asp, Glu containing nacre-specific protein sequences also demonstrated that the global structure of these sequences are not conformationally transformed by the presence of Ca (II).[21]

DISCUSSION

In a previous study, we utilized AFM microscopy to monitor the effects of nacreous protein sequences (AP7N, AP24N, n16N) on calcite hillock growth, wherein we uncovered evidence of multifunctionality within this series of polypeptides.[17] In the present study, we have now extended our observations to a different family of biomineralization protein sequences, a subset found in the prismatic layer – associated protein superfamily, Asprich.[12,15] Here, we observe that the highly conserved 42 AA C-terminal domain transforms calcite hillock growth kinetics and morphology. Specifically, this C-terminal domain promotes the formation of clusters and voids on hillock terrace surfaces (Figure 2), and subsequently pins acute step edges (Figures 2, 3), limits obtuse step motion (Figure 5), and alters the morphology of acute – obtuse corner regions and promotes emergence of new step directions (Figures 2, 3), leading to the formation of a rounded hillock geometry (Figures 3, 7). The net result is a "tuning" of crystal morphology and growth that shares some features with the nacre scenario: Fragment-2 and nacreous AP7N, AP24N pin acute

steps and induce cluster deposits on terrace surfaces,[17] although probable differences in the nature of the clusters have yet to be determined. In addition, n16N, like Fragment-2, also generates new step directions and modified acute-obtuse corner morphologies.[17] In addition to these similarities, there are also important functional differences which distinguish Fragment-2 from the nacreous polypeptides. Unlike Fragment-2, both AP7N and AP24N promote obtuse step acceleration and preservation of rhombohedral morphology and do not introduce voids.[17] These functional similarities and differences most likely arise from some combination of sequence and structural characteristics that are found within these polypeptides.[15,17] It remains to be seen if these functional and structural trends will hold true for other nacre- and prismatic-associated polypeptides as well.

The phenomena of acceleration or deceleration of calcite step velocities have been observed for several systems, including nacre-associated AP7N, AP24N,[17] other nacre proteins[23] and aspartic acid – rich sequences.[24] Acceleration is also observed for Fragment-2 and its associated subdomains, where obtuse step velocities were observed to increase (approximately 2x) near the dislocation source relative to the negative control (Figure 5). The mechanism by which peptides promote increased step kinetics is uncertain, but several effects have been postulated, including changes in the activation barriers associated with moving ions from solution to the solid phase and local changes in supersaturation.[17,23] Additionally, the step velocity increase observed at low additive concentrations can be attributed to an increase in kink density created by impurity interactions.[25,26] However, unlike the nacreous polypeptides,[17] Asprich-associated sequences also induce a transient acceleration phase, and as the steps continue to propagate further from the dislocation source, deceleration occurs (Figure 5). This inhibition would be expected for steps

interacting with increasing concentrations of pinning sites and may occur either because the step has more time to interact with the solubilized polypeptide, or, because the step traverses across the terrace-bound polypeptide. Eventually, fewer growth sites are present and high step curvature develops and this combination acts to pin the steps rather than accelerate them.[25] Interestingly, the mixture of Acidic-2 and DEAD-17, which has the same amino acid constituents as Fragment-2, has the greatest inhibitory effect on step velocity (Figure 5). This may be because the mixture has twice as many "blocker" species, although each has a smaller sequence length and molecular mass.

Our present AFM study takes us a step further from our original SEM studies of Fragment-2,[15] and illustrates several interesting phenomena with regard to the functional contributions and mineralization behavior of the DEAD-17 and Acidic-2 subdomains with respect to Fragment-2. In this study there are three basic morphological effects that are observed in the presence of C-terminal – associated Asprich sequences: loss of rhombohedral morphology and emergence of new step directions, wandering of steps, and cluster formation on the terraces. As shown in Figures 2, 3, and 7, the acute step pinning and cluster formation phenomena are observed in the presence of Fragment-2 or Acidic-2, but not with DEAD-17. Conversely, the extent of morphological variation and the kinetics of step growth in the presence of Fragment-2 appear to correlate more closely with DEAD-17 traits as opposed to those of Acidic-2 (Figure 3, 7). Hence, each subdomain appears to contribute a specific mineralization trait to the parent domain. But what is even more intriguing is the fact that the individual mineralization traits of the DEAD-17 and Acidic-2 undergo a metamorphosis when both domains are present together, either as colinear partners (Fragment-2, Figures 3C, 7) or simultaneously as individual species (Figures 3D, 7).

Specifically, we note the following: (a) Fragment-2 induces a round hillock morphology, whereas the individual Acidic-2 and DEAD-17 subdomains induce a more oval morphology (Figure 7) and the 1:1 subdomain mixture induces an irregular polygonal form; (b) the individual Acidic-2 subdomain inhibits obtuse step velocities to a greater degree than Fragment-2, and, the 1:1 mixture of the individual Acidic-2 and DEAD-17 subdomains exhibits the highest degree of velocity inhibition. Although the reasons for these phenomena still elude us, we suspect that there is some interactive participation between subdomains, and it appears that this interplay changes when one moves from a intramolecular arrangment (Figure 3C) to a dispersed mixture scenario (Figure 3D). If true, then sequence interplay may represent a general phenomenon in biomineralizing systems, i.e., a specific effect on crystal growth and nucleation is achieved by the interplay of several sequences within an intra- or intermolecular context. Additional investigations will be required to assess how widespread sequence interplay may be in protein-based biomineralization.

Finally, in light of our present findings, we would like to comment on our original observations of Fragment-2 - induced porosity formation in calcite crystals *in vitro*,[15] and, the potential impact that the conserved C-terminal sequence may have on Asprich-mediated prismatic calcite crystal formation in the mollusk. Our AFM findings indicate that Fragment-2 induces step roughening at obtuse step edge regions of calcite crystals (Figure 3). This uneven growth leads to the formation of two dimensional "finger-like" regions (Figures 3, 4), where some degree of crystal growth occurs right next to a region that is lagging, leading to the formation of repetitive "finger – void" regions at the mineralization front. It is not unlikely that this pattern is replicated in three dimensions, leading to the presence of void

regions where crystal growth cannot keep up with the advancing mineralization front.. Additionally, we have also observed void formation arising as a result of surface roughening induced by cluster formation (Figure 2). Collectively, these observations offer two possible pathways that lead to void or pore formation and may help to explain why we initially observed voids or pores on the surfaces of micron-sized calcite crystals.[15] Given that prismatic calcite arrays are limited in cross-sectional dimension within the prismatic layer of the mollusk,[9,11] we speculate that one potential function of Asprich may be to limit crystal dimensions during mollusk shell development. If true, then the 42 AA C-terminal domain region may participate in this process to some degree. Additional studies will be required to determine how these specific sequences participate in the crystal growth and design of prismatic calcite arrays in the mollusk shell.

ACKNOWLEDGMENTS This work was supported by funding from the Department of Energy (DE-FG02-03ER46099, to JSE). Portions of this work were performed under the auspices of the U.S. Department of Energy by the University of California, Lawrence Livermore National Laboratory under Contract W-7405-Eng-4. This paper represents contribution number 35 from the Laboratory for Chemical Physics, New York University. This work was performed under the auspices of the DOE byUC, LLNL under Contract W-7405-Eng-48.

REFERENCES

1. Aizenberg, J., Albeck, S., Weiner, S., and Addadi, L. (1994) *J. Cryst. Growth* **142**: 159-164.

2. Aizenberg, J., Thachenko, A., Weiner, S., Addadi, L., Hendler, G. (2001) *Nature* **412**: 819-822.

3. (a) Belcher, A.M., Wu, X.H., Christensen, R.J., Hansma, P.K., Stucky, G.D., Morse, D.E. (1996) *Nature* **381**: 56-59; (b) Falini, G., Albeck, S., Weiner, S., Addadi, L. (1996) *Science* **271**: 67-69.

4. (a) Weiss, I.M., Tuross, N., Addadi, L., Weiner, S. (2002) *J. Exptl. Zool.* **293**: 478-491; (b) Addadi, L., Raz, S., Weiner, S. (2003) *Adv. Mater.* **15**: 959-970; (c) Nassif, N., Pinna, N., Gehrke, N., Antonietti, M., Jager, C., Colfen, H. (2005) *Proc. Natl. Acad. Sci USA* **102**: 12653-12655.

5. Smith, B.L., Schaffer, T.E., Viani, M., Thompson, J.B., Frederick, N.A., Kindt, J., Belcher, A., Stucky, G.D., Morse, D.E., Hansma, P.K. (1999) *Nature* **399**: 761-769.

6. Li, X., Chang, W.C., Chao, Y.J., Wang, R., Chang, M. (2004) *Nano Let* **4**: 613-617.

7. Eichhorn, S.J., Scurr, D.J., Mummery, P.M., Golshan, M., Thompson, S.P., Cernika, R.J. (2005) *J. Mat. Chem.* **15**: 947-952.

8. Shen, X., Belcher, A.M., Hansma, P.K., Stucky, G.D., Morse, D.E. (1997) *J. Biol. Chem.* **272**: 32472-32481.

9. Marin, F., Amons, R., Guichard, N., Stigter, M., Mecker, A., Luquet, G., Layrolle, P., Alcaraz, G., Riondet, C., Westbroek, P. (2005) *J. Biol. Chem* **280**: 33895-33908.

10. Dauphin, Y., Curif, J.P., Doucet, J., Salome, M., Susini, J., Williams, C.T. (2003) *Marine Biology* **142**: 299-304.

11. Pokroy, B., Fitch, F.N., Marin, F., Kapon, M., Adir, M., Zolotoyabko, E. (2006) *J. Struct. Biol* **155**: 96-103.

12. Gotliv, B.-A., Kessler, N., Sumerel, J.L., Morse, D.E., Tuross, N., Addadi, L., Weiner, S. (2005) *Chem. Bio. Chem.* **6**: 304-314.

13. Tsukamoto, D., Sarashina, I., Endo, K. (2004) *Biochem. Biophys. Res. Commun.* **320**: 1175-1180.

14. Suzuki, M., Murayama, E., Inoue, H., Ozaki, N., Tohse, H., Kogure, T., Nagasawa, H. (2004) *Biochem. J.* **382**: 205-213.

15. Collino, S., Kim, I.W., Evans, J.S., (2006) *Cryst. Growth Des.*, **6:** 839-842.

16. Initially, we named the 42 AA C-terminal domain "DEAD-Acidic-2". However, to avoid confusion with the individual subdomain names, we have chosen to rename the 42 AA sequence "Fragment-2".

17. Kim, I.W., Darragh, M.R., Orme, C., Evans, J.S. (2006) *Cryst. Growth Des.*, **5**: 5-10.

18. Teng, H.H., Dove, P.M., Orme, C.A., De Yoreo, J.J. (1998) *Science* **282:** 724-728.

19. Kim, I.W., DiMasi, E., Evans, J.S. (2004) *Cryst. Growth Des.*, **4**: 1113-1118.

20. Michenfelder, M., Fu, G., Lawrence, C., Weaver, J.C., Wustman, B.A., Taranto, L., Evans, J.S., and Morse, D.E., (2003) *Biopolymers* **70**: 522-533; errata 73: 299.

21. Kim, I.W., Morse, D.E., and Evans, J.S. (2004) *Langmuir* **20**: 11664-11673.

22. (a) Cubelis, M.V., Caillez, F., Blundell, T.L., Lovell, S.C. (2005) *Proteins: Struct. Func. Bioinform*. **58**: 880-892; (b) Chellgren, B.W., Creamer, T.P. (2004) *Biochemistry* **43**: 5864-5869; (c) Eker, F., Griebenow, K., Cao, X., Nafie, L.A., Schweitzer-Stenner, R. (2004) *Biochemistry* **43**: 613-621.

23. Fu, G., Qiu, S. R., Orme, C. A., Morse, D. E. & De Yoreo, J. J. (2005) *Adv. Mat.* **17**, 2678-2684.

24. Elhadj, S., Salter, E.A., Wierzbicki, A., De Yoreo, J.J., Han, N., Dove, P.M. (2006) *Cryst. Growth Des.*, **6**: 197-201.

25. Cabrera, N., Vermilyea, D.A., in *Growth and Perfection of Crystals* (eds. Doremus, R.H., Roberts, B.W., Turnbull, D.) pg. 393. Wiley, 1958.

26. Sangwal, K., (1996) *Prog. Crystal Growth and Charact.* **32**: 3-43.

27. The energy required to create a kink in sparingly soluble minerals such as calcite is relatively high (E/kT ~2.4)[25,26] which implies that kink nucleation is likely the rate-limiting step for step growth, giving credence to this proposed scenario.

Figure Legends for Kim *et al* 2007

Figure 1: Primary sequence of Asprich C-terminal 42 AA Fragment 2 and associated subdomains.

Figure 2: *AFM images of calcite dislocation hillock regions in the presence of Fragment-2.* (**A**) negative control (no peptide added); (**B**) 3 μM Fragment-2; (**C**) 6 μM Fragment-2; (**D**) dry topographical image of terrace surfaces after exposure to 6 μM Fragment-2, revealing clusters (rough areas) and voids (dark areas) on crystal surface. All images are shown in the same orientation as (A), with the two acute steps at the top of the images. Scalebars indicate dimensions.

Figure 3: *AFM images of the dislocation hillock region of calcite crystals.* (**A**) DEAD-17 subdomain (note presence of two hillocks); (**B**) Acidic-2 subdomain; (**C**) Fragment-2 domain (insert image size is 5 μm x 5 μm); (**D**) 1:1 mole mixture, Acidic-2 and DEAD-17 subdomains. In A – D, total peptide concentration = 12 μM. All images are shown in the same orientation as (A), with the two acute steps at the top of the images. AFM inset images are those recorded immediately prior to the introduction of each peptide. Scalebars indicate image dimensions.

Figure 4: *Sequential AFM images showing "finger" formation on dislocation hillock in the presence of Acidic-2* All images are shown in the same orientation and dimensions as in Figure 2C. Black and white arrows indicate different regions on hillock where emergence of "finger" extensions are noted.

Figure 5: *Obtuse – obtuse corner velocities determined for* (**A**) *Fragment-2,* (**B**) *DEAD-17,* (**C**) *Acidic-2,* (**D**) *1:1 DEAD-17 : Acidic-2 mixture*. Open circle = 12 μM, black circle = 6 μM peptide concentration. Gray line indicates velocity range observed for the obtuse – obtuse corner prior to introduction of each peptide (i.e., negative control scenario).

Figure 6: *Circular dichroism spectra of* (**A**) Fragment-2, (**B**) Acidic-2, (**C**) DEAD-17 *in 100 μM Tris-HCl, pH 7.5 buffer.* Apo and peptide : Ca (II) stoichiometries are denoted in each CD plot. All peptide concentrations = 12 μM.

Figure 7: *Summary of Asprich C-terminal domain and subdomain effects on dislocation hillock regions of calcite.* Here, an idealized calcite hillock region is portrayed at the top of the figure, and events occuring at the acute and obtuse steps, cluster formation, as well as overall morphology features (not drawn to scale), are noted for (**A**) Fragment-2, (**B**) DEAD-17; (**C**) Acidic-2; (**D**) 1:1 Acidic-2 : DEAD-17 mixture. HSF = hillock shape factor, calculated as described in Materials and Methods. Note that, with respect to the idealized hillock, the polypeptide-affected terrace boundaries are roughened in a relative fashion to represent the degree of irregular features that are observed in our AFM images.

145 186

...DEADEADADEADADEADADNDAADETDAADVGTEAEDVADDE

DEAD17 **Acidic-2**

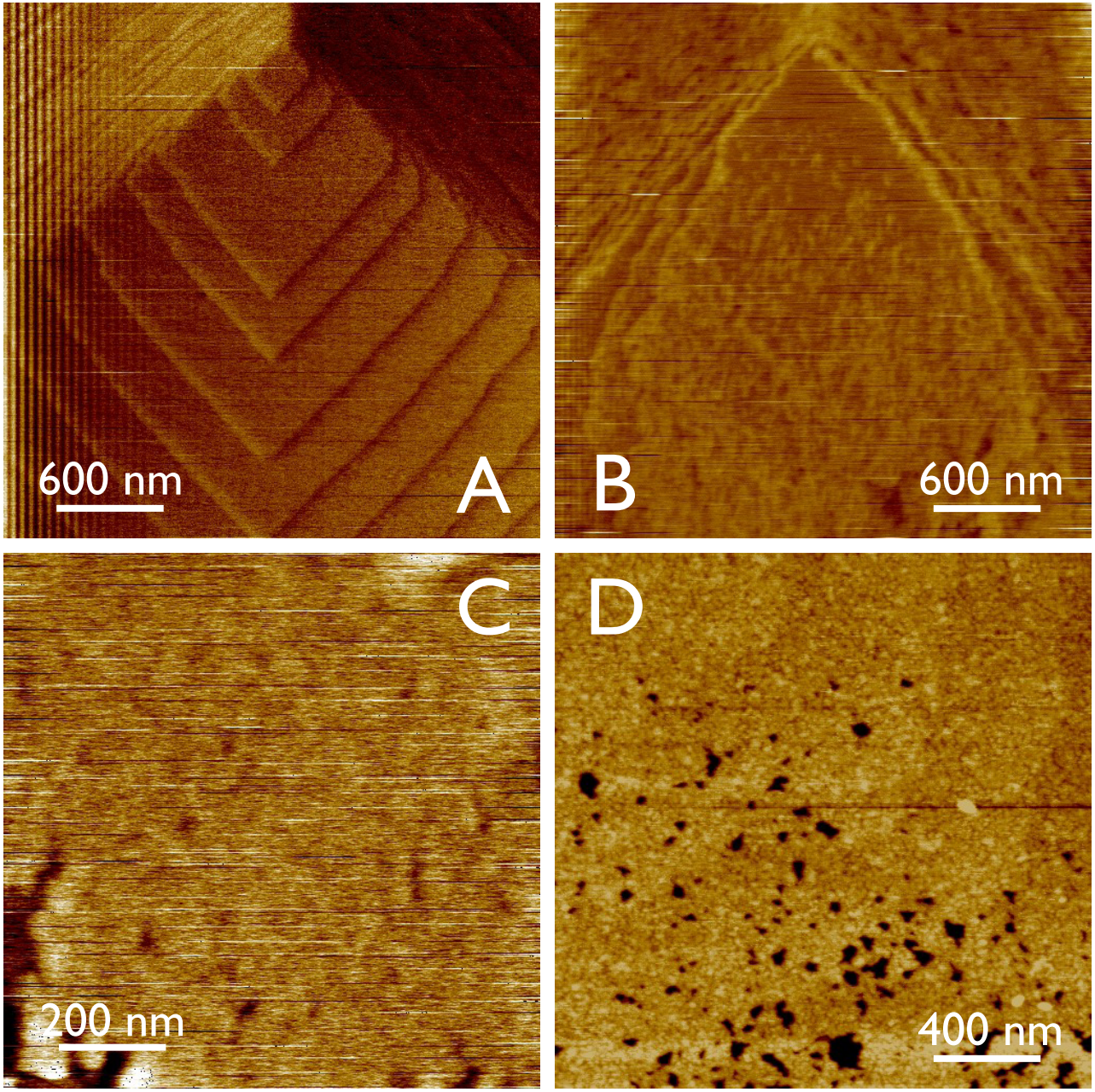
600 nm
A
B
600 nm
C
200 nm
D
400 nm

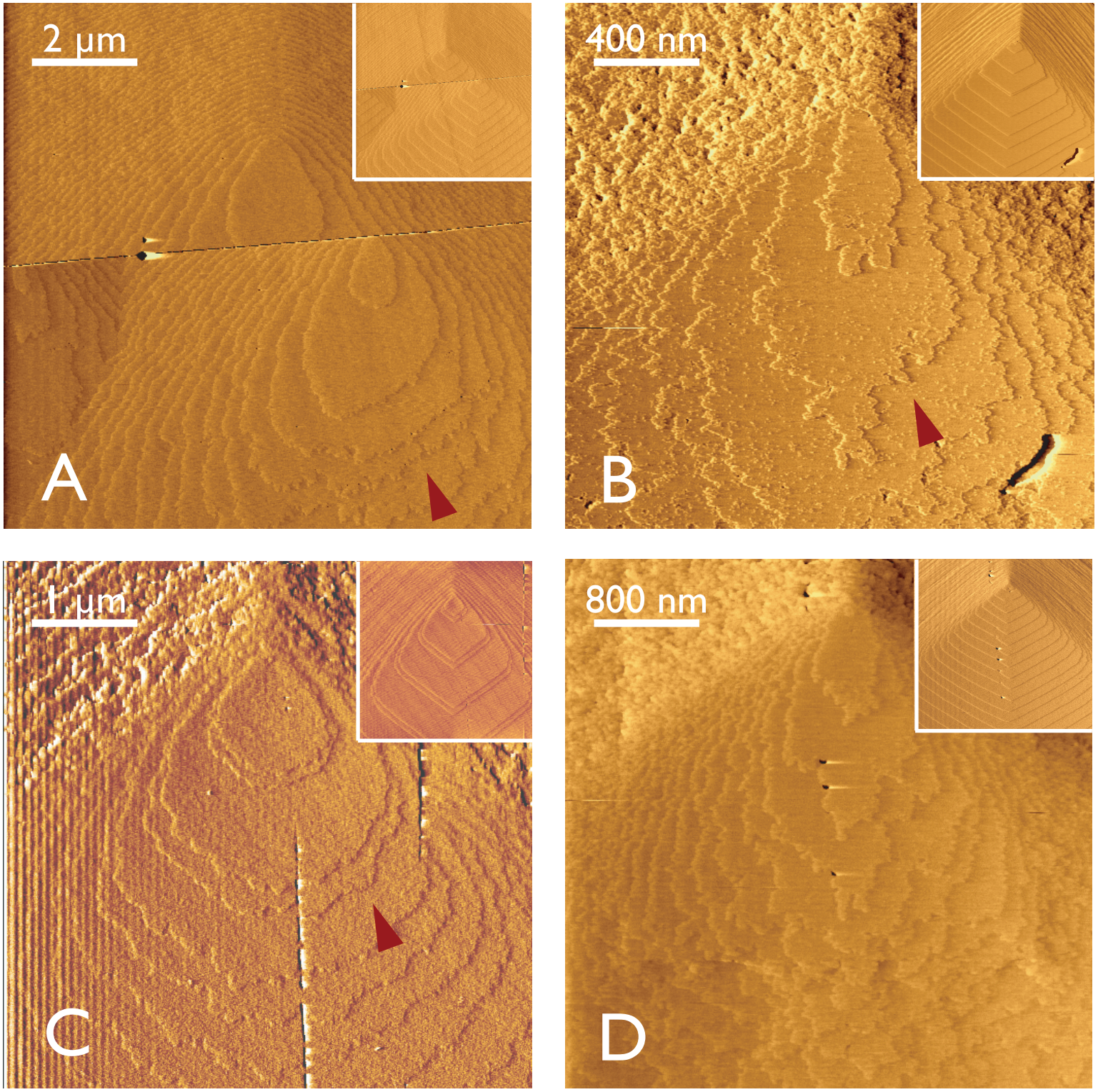
2 µm
A
400 nm
B
1 µm
C
800 nm
D

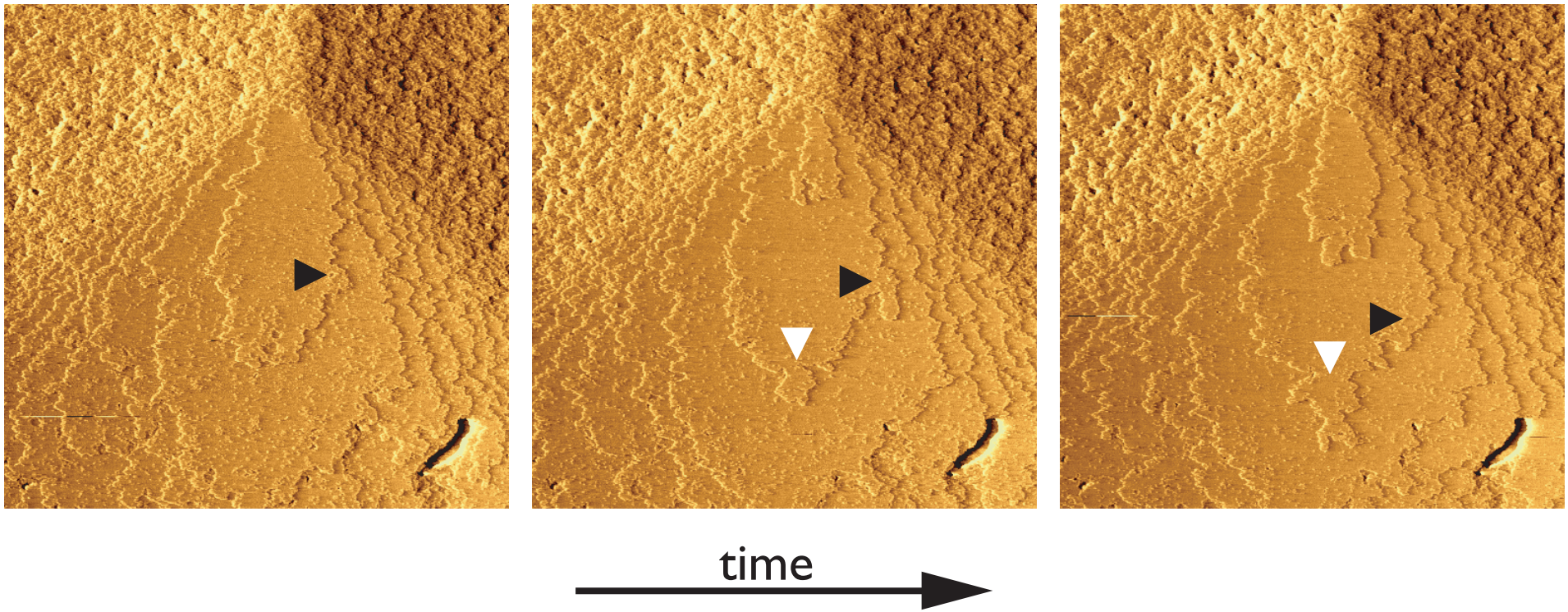
time

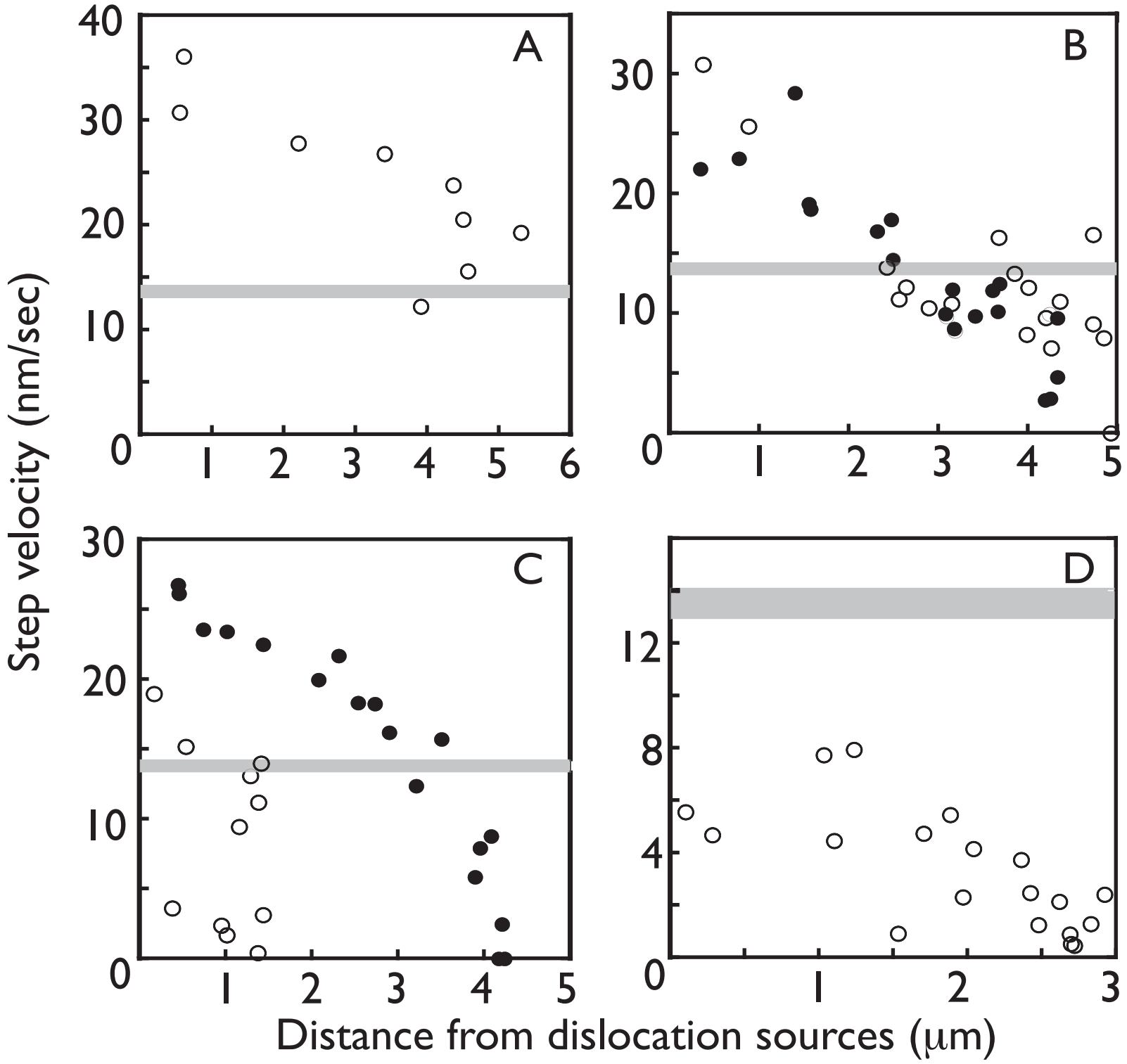
A
B
C
D
Step velocity (nm/sec)
Distance from dislocation sources (μm)

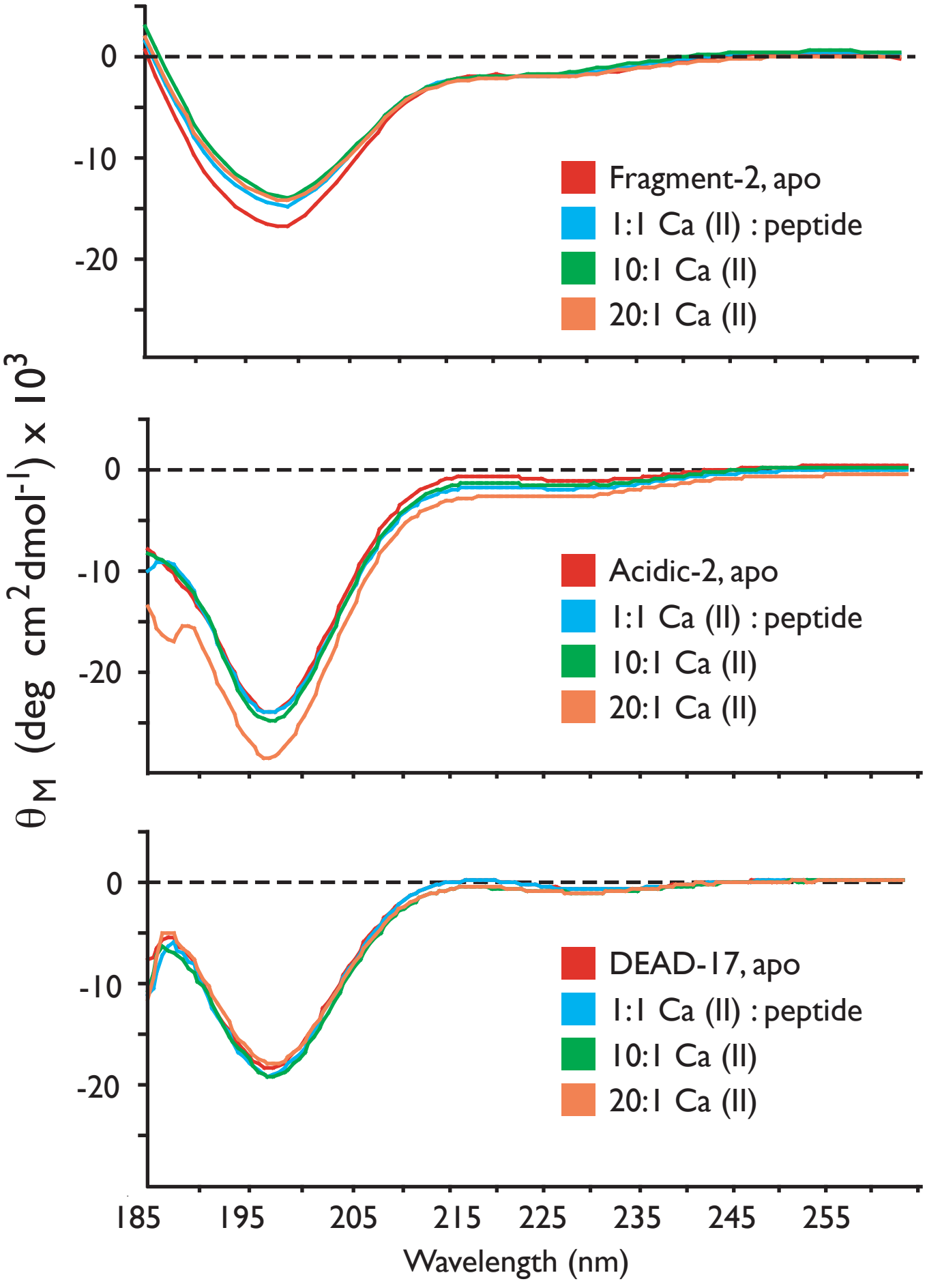
0
-10
-20
Fragment-2, apo
1:1 Ca (II) : peptide
10:1 Ca (II)
20:1 Ca (II)
0
-10
-20
Acidic-2, apo
1:1 Ca (II) : peptide
10:1 Ca (II)
20:1 Ca (II)
0
-10
-20
DEAD-17, apo
1:1 Ca (II) : peptide
10:1 Ca (II)
20:1 Ca (II)
185
195
205
215
225
235
245
255
Wavelength (nm)
θM (deg cm2dmol-1) x 10^3

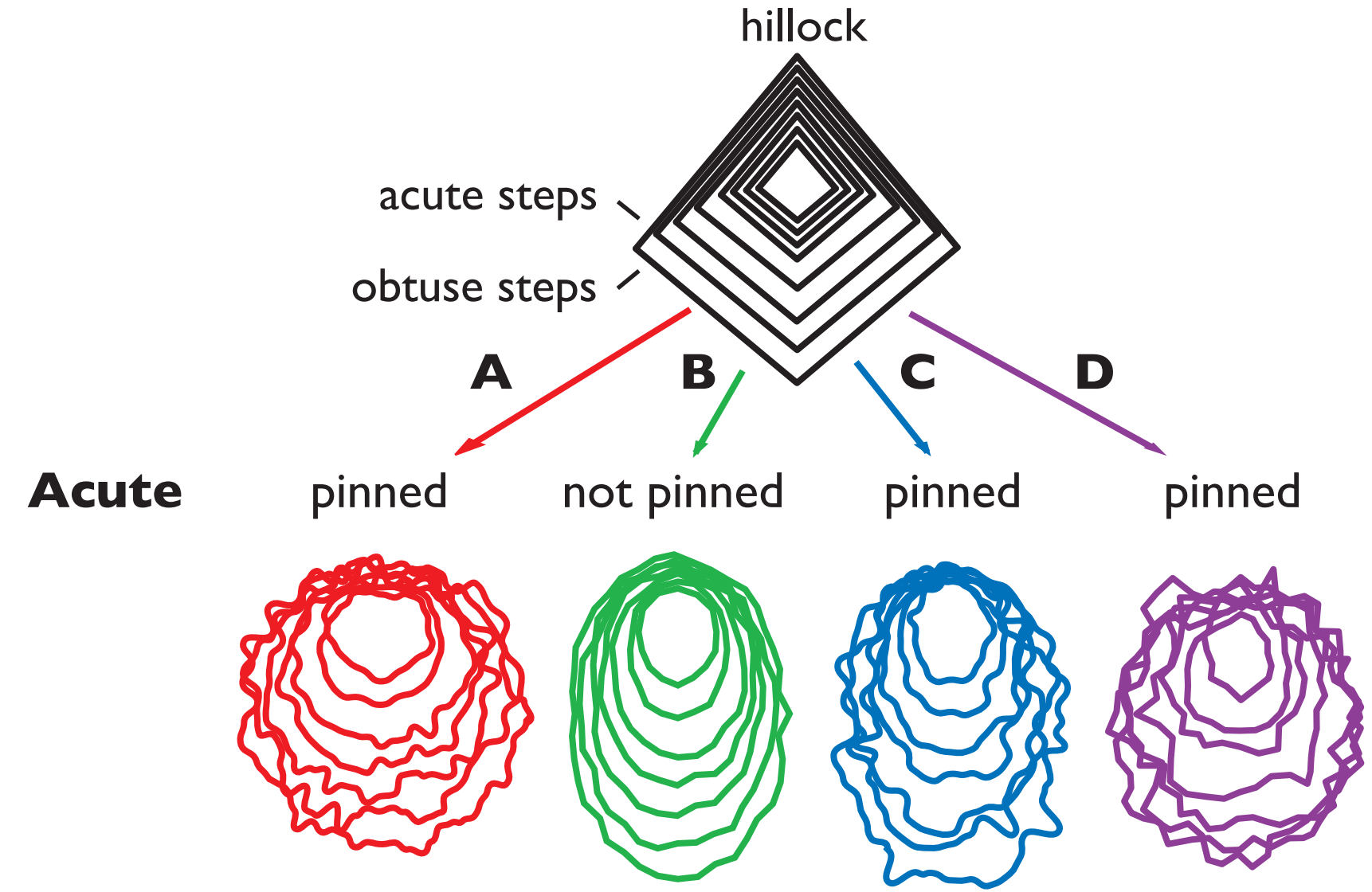
hillock
acute steps
obtuse steps
A
B
C
D
Acute
pinned
not pinned
pinned
pinned
Clusters
(+)
(-)
(+)
(+)
HSF
1.1
1.3
1.9
1.8
Shape
round
oval
elongated oval
polygonal